

## Core Shell Structures in Comparative Study of the Composition $x = 0.01$ ( $\text{BaTi}_{1-5x}\text{Nb}_{4x}\text{O}_3$ ) Prepared by the Barium Titanate Route and the Solid-state Route

Alberto Arenas-Flores<sup>1</sup>, Martín Ortiz-Domínguez<sup>2\*</sup>, Oscar Gómez-Vargas<sup>3</sup>, José Solís-Romero<sup>3</sup>, Ángel Jesús Morales-Robles<sup>1</sup>, Arturo Cruz-Avilés<sup>2</sup>, Ángelica Viridiana Duran-Sarabia<sup>2</sup>, Edgar Cardoso-Legorreta<sup>1</sup> and Jorge Zuno-Silva<sup>2</sup>

<sup>1</sup> AACTyM, Universidad Autónoma del Estado de Hidalgo, Mineral de la Reforma, Hidalgo, Mexico

<sup>2</sup> Department of Mechanical Engineering, Universidad Autónoma del Estado de Hidalgo, Ciudad Sahagún, Hidalgo, Mexico

<sup>3</sup> Postgraduate Division, Instituto Tecnológico de Tlalnepantla, Estado de México, México.

\* Corresponding author: martin\_ortiz@uaeh.edu.mx

Barium titanate ( $\text{BaTiO}_3$ ) is known that the addition of small amount of  $\text{Nb}^{5+}$  has significant effects on the bulk electrical properties and widespread applications [1, 6]. At room temperature has a tetragonal perovskite structure, during sintering it transforms to the cubic paraelectric state and undoped  $\text{BaTiO}_3$  is electrically insulating, but oxygen deficiency can occur at high temperatures ( $>1350^\circ\text{C}$ ) and or in reducing atmospheres [7]. However, how  $\text{Nb}^{5+}$  is distributed locally and its incorporation and diffusion in barium titanate and what structural variations it causes have not been studied in depth. There are several discrepancies in properties of  $\text{Nb}^{5+}$  incorporation into  $\text{BaTiO}_3$  and have been reported in literature [8], these complications appears to consists in a slow rate of  $\text{Nb}^{5+}$  incorporation into the  $\text{BaTiO}_3$  lattice and also a narrow temperature range at which the incorporation is effective. Diffuse phase transition (DPT) behavior was observed in  $\text{BaTiO}_3$  samples with additions of Zr, Cd, Bi and Nb, the microstructure of these ceramic was characterized by a core-shell structure [9] which featured a core and shell for ferroelectric and paraelectric phases respectively. It was suggested that the core and shell are not different phases [9]. During sintering a core-shell structure can be developed as a result of densification and grain growth which were assisted by a liquid phase [9]. It was further suggested that core-shell structure tends to disappear at high temperatures [9]. In this study, we report characteristic core-shell structure, also, chemical inhomogeneity is found as a result of (DPT). According to this in mind, in this work, X ray diffraction, electrical measurements, scanning electron microscope and transmission electron microscope studies were used to investigate the  $\text{BaTiO}_3$  system with  $\text{Nb}^{5+}$  dopant by two different routes called mixed oxide route and barium titanate route with barium carbonate and barium titanate as initial reagents respectively, to determine effects on physical properties. The synthesis and characterization of compositions based on the titanium vacancy mechanism  $\text{BaTi}_{1-5x}\text{Nb}_{4x}\text{O}_3$  (B-site vacancies) with  $x = 0.01$  was investigated. Compositions were prepared by the conventional solid state (mixed oxide route and BT route). All reagents were dried at appropriate temperatures, between 200 and  $600^\circ\text{C}$ . Raw materials were then weighed using a 5 decimal place, precise balance, according to the stoichiometric formula of the desired composition. Appropriate amounts of reagents ( $\text{BaCO}_3$ ,  $\text{Nb}_2\text{O}_5$  and  $\text{TiO}_2$ ) were mixed either for  $\sim 25$  minutes in acetone using an agate mortar and pestle until dry. Stoe diffractometer was used to collect X-ray diffraction data: using a linear position sensitive detector (PSD). The synthesis and characterization of compositions based on the titanium vacancy mechanism  $\text{BaTi}_{1-5x}\text{Nb}_{4x}\text{O}_3$  (B-site vacancies) with  $x = 0.01$  was investigated. Compositions were prepared by the conventional solid state (mixed oxide route and BT route). All reagents were dried at appropriate temperatures, between 200 and  $600^\circ\text{C}$ . Raw materials were then weighed using a 5 decimal place, precise balance, according to the stoichiometric formula of the desired composition. Appropriate amounts of reagents ( $\text{BaCO}_3$ ,  $\text{Nb}_2\text{O}_5$  and  $\text{TiO}_2$ ) were mixed either for  $\sim 25$  minutes in acetone using an

agate mortar and pestle until dry. Stoe diffractometer was used to collect X-ray diffraction data: using a linear position sensitive detector (PSD). In Figure 1, XRD data are presented for a sample with  $z = 0.01$  prepared by the BT route which was made from pre-prepared  $\text{BaTiO}_3$ . This sample was fired at several temperatures below  $1550^\circ\text{C}$ ; in all cases, a cubic product phase was obtained. However, when the sample was heated at  $1550^\circ\text{C}$ , the formation of mixed hexagonal (JCPDS 340129) and cubic (JCPDS 310174) phases was evident. The SEM micrograph shown in Figure 2 was obtained on the sample sintered at  $1550^\circ\text{C}$ ; due to use of a high sintering temperature, under SEM (Figure 2) an inhomogeneous morphology of the pellet was observed, two different regions can be seen: labeled as “a” and “b”. Region “a” has a characteristic of typically liquid phase region, which has a large and uniform grain size greater than  $10\ \mu\text{m}$ , and a region “b” has a small grain size. It is clear from Figure 2 that there is a bimodal distribution of large grains in a fine-grain matrix. This liquid phase region probably contains a mixture of two phases, cubic (small grain size) and cubic + liquid (liquid phase). TEM bright-field images are shown in Figure 3a, 3b, 3c and 3d. In Figure 3a, a typical core-shell structure is shown with a core region encircled by a shell. The shell-core structure of grains is composed of two different regions: a grain core, which is ferroelectric and contains principally barium titanate and the non-ferroelectric (paraelectric) region, which is rich in  $\text{Nb}^{5+}$ . The occurrence of a shell-core structure in this sample is a result of inhomogeneous distribution of  $\text{Nb}^{5+}$  in the barium titanate. Figure 3b shows details of the core-shell structure and the ferroelectric domains can clearly be observed. In addition, in this material a network of dislocations was found and is shown in Figure 3c. An enlarged section of the core region is presented in Figure 3d. XRD results clearly demonstrate that when the sample prepared under BT route was heated at temperatures of  $1550^\circ\text{C}$  a second phase appeared which was identified, as hexagonal  $\text{BaTiO}_3$ . It was clear by XRD that in samples prepared by BT route the cubic phase could be obtained at temperatures up to  $1500^\circ\text{C}$ , without any evidence of secondary phases. TEM results showed that the core and shell structure result due to an inhomogeneous distribution of  $\text{Nb}^{5+}$  inside the barium titanate in sample prepared under BT route, consequently, this has an important role on the temperature dependence of the dielectric constant.

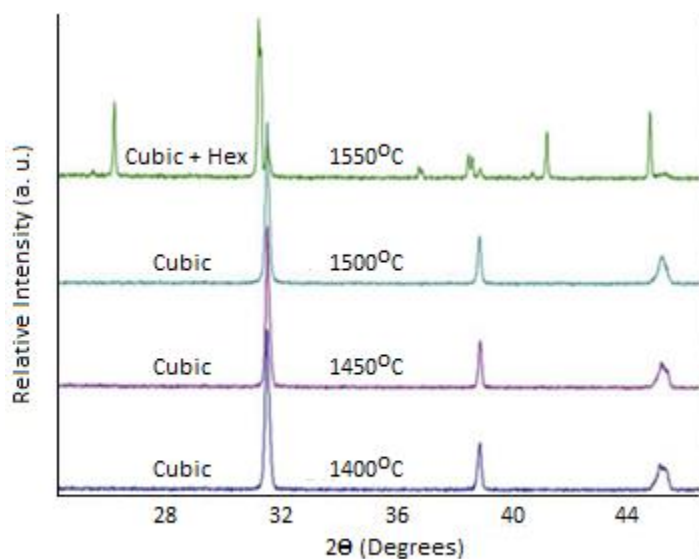


Fig. 1

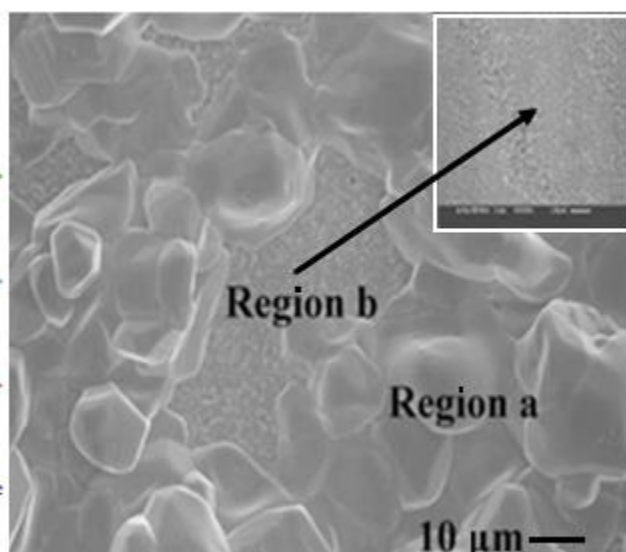
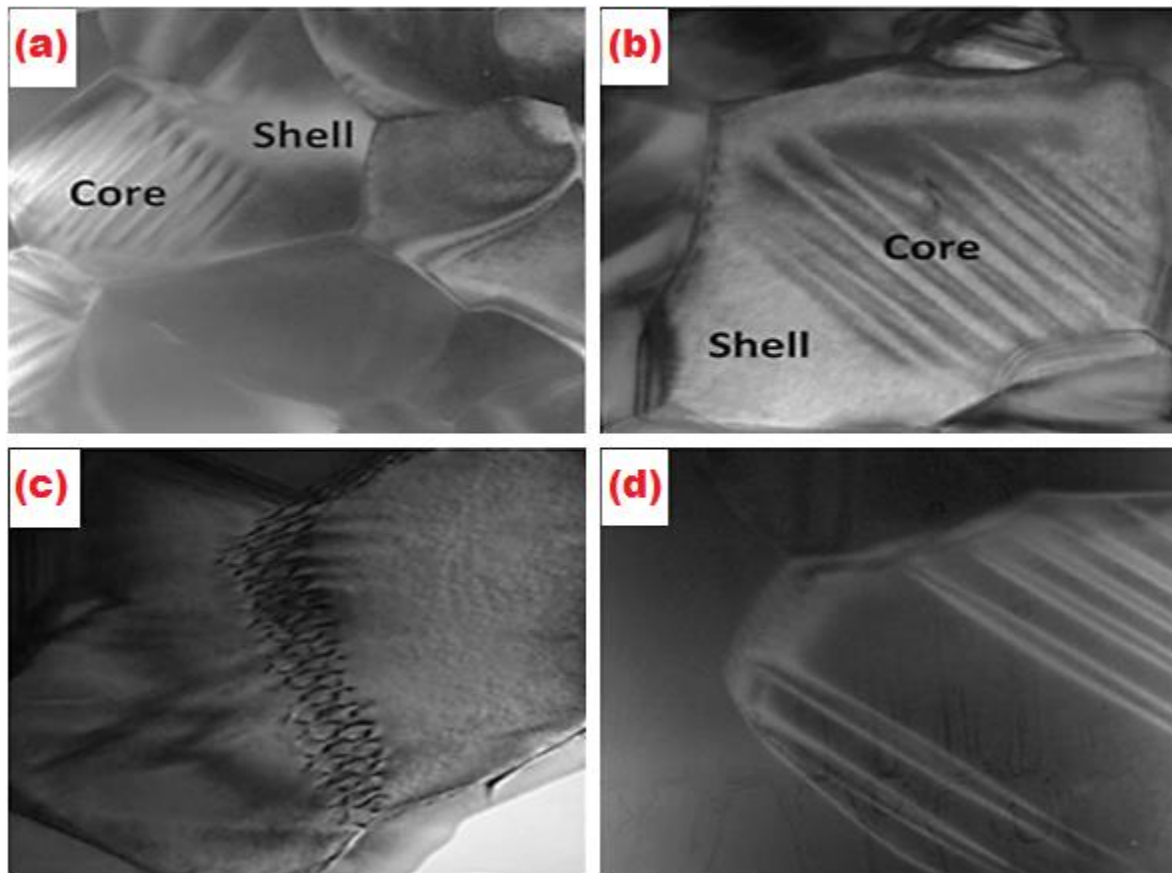


Fig. 2

**Figure 1.** XRD data for sample with  $x = 0.01$  prepared by the BT route. SEM micrograph for sample prepared by BT route heated at (Figure 2).



**Figure 3.** TEM bright-field images are shown in (a), (b), (c) and (d) for composition with  $x = 0.01$  prepared by.

#### References:

- [1] S. Wang, S. Zhang, X. Zhou, B. Li, Z. Chen, *Mater. Lett.* **60** (2006) 909-911. <https://doi.org/10.1016/j.matlet.2005.10.043>
- [2] K. Kowalski, M. Ijjaali, T. Bak, B. Dupre, J. Nowotny, M. Rekas, C. C. Sorrell, *J. Phys. Chem. Solids*, **62** (2001) 531-535. [https://doi.org/10.1016/S0022-3697\(00\)00211-0](https://doi.org/10.1016/S0022-3697(00)00211-0)
- [3] E. Brzozowski, M. S. Castro, C. R. Foschini, B. Stojanovic, *Ceram. Int.* **28** (2002) 773-777. [https://doi.org/10.1016/S0272-8842\(02\)00042-1](https://doi.org/10.1016/S0272-8842(02)00042-1)
- [4] F. R. Barrientos Hernández, A. Arenas Flores, E. Cardoso Legorreta, *Integr. Ferroelectr.* **126** (2011) 1-6. <https://doi.org/10.1080/10584587.2011.574963>
- [5] F. R. Barrientos Hernández, I. A. Lira Hernández, C. Gómez Yáñez, A. Arenas Flores, R. Cabrera Sierra, M. Pérez Labra, *J. Alloy. Comp.* **583** (2014) 587-592. <https://doi.org/10.1016/j.jallcom.2013.09.016>
- [6] M. E. Lines, A. M. Glass in "Principles and Applications of Ferroelectrics and Related Materials" Oxford University Press Editor, (Oxford, UK) p.696.
- [7] O. Saburi, *J. Phys. Soc. Jpn.* **14** (9) (1959) 1159-1174. <https://doi.org/10.1143/JPSJ.14.1159>
- [8] W. R. Buessem, M. Kahn, *J. Am. Ceram. Soc.* **54** (9) (1971) 458-461. <https://doi.org/10.1111/j.1151-2916.1971.tb12385.x>
- [9] D. Hennings and R. Rosenstein, *J. Am. Ceram. Soc.* **67** (4) (1984) 249-254. <https://doi.org/10.1111/j.1151-2916.1984.tb18841.x>